The Resistance and EEDI Analysis of Trimaran Vessel with and without Axe-bow

Analiza otpora i EEDI-a trimarana sa i bez sjekirastog pramca

Richard Benny Luhulima*
Universitas Pattimura
Department of Naval Architechture
E-mail: richardluhulima26@gmail.com

Sutiyo
Universitas Hang Tuah
Department of Naval Architechture
E-mail: sutiyo@hangtuah.ac.id

I Ketut Aria Pria Utama
Institut Teknologi Sepuluh Nopember
Department of Naval Architechture
E-mail: kutama@na.its.ac.id

DOI 10.17818/NM/2022/3.1
UDK 502/504:656.61
620.9
Preliminary communication / *Prethodno priopćenje*
Paper received / *Rukopis primljen:* 28. 7. 2021.
Paper accepted / *Rukopis prihvaćen:* 11. 5. 2022.

Abstract

Efforts to reduce emission of toxic gases into the atmosphere by sea transportation have been consistently carried out by the International Maritime Organisation (IMO) since 2009. IMO has introduced a regime known as energy efficiency design index (EEDI) to monitor and quantify the emission of CO_2 because of its global climate impact. A comparison was conducted between trimaran hull forms without and with Axe-Bow on the main-hull with S/L=0.3 and 0.4, as well as a comparison with a monohull of comparable displacement. The CFD method was used to analyse resistance. Overall, the trimaran without the Axe-Bow can decrease resistance by 22.6%, while the trimaran with the axe-bow can reduce resistance by 25.0%. Additionally, this resulted in a 54.8% decrease in EEDI on trimarans without axe-bow and a 55.4% reduction on trimaran equipped with axe-bow when compared to MV Sabuk Nusantara 104. In addition, despite little difference between trimaran with and without axe-bow, the introduction of axe-bow has shown apparent benefits to lower EEDI.

KEY WORDS

Trimaran
Axe-Bow
Monohull
IMO
EEDI
CO_2 emission

Sažetak

Od 2009. godine Međunarodna pomorska organizacija (IMO) dosljedno ulaže napore u smanjenje emisije otrovnih plinova u atmosferu uzrokovane pomorskim prometom. IMO je uveo projektni indeks energetske učinkovitosti (EEDI) za praćenje i kvantificiranje emisije CO_2 s obzirom na globalni klimatski utjecaj. Provedena je usporedba između oblika trupa trimarana sa i bez sjekirastog pramca (Axe-Bow) na glavnom trupu sa S/L=0,3 i 0,4, kao i usporedba s jednotrupcem usporedive istisnine. Za analizu otpora korištena je računalna dinamika fluida. Trimaran bez sjekirastog pramca može smanjiti otpor za 22,6 %, dok trimaran sa sjekirastim pramcem može smanjiti otpor za 25,0 %. To je rezultiralo smanjenjem EEDI-ja od 54,8 % na trimaranima bez sjekirastog pramca i smanjenjem od 55,4 % na trimaranu sa sjekirastim pramcem u usporedbi s MV Sabuk Nusantara 104. Unatoč malim razlikama između trimarana sa i bez sjekirastog pramca, njegovo uvođenje pokazalo je očite prednosti za niži EEDI.

KLJUČNE RIJEČI

trimaran
sjekirasti pramac
jednotrupac
IMO
EEDI
emisija CO_2

1. INTRODUCTION / *Uvod*

Maritime transport remains the backbone of global transportation on a worldwide scale due to the high volume of goods carried by large ships and the cheap unit transportation costs compared to air transportation. Approximately 80% of world trade by volume and 70% by value is carried by sea and handled by ports [1]. Over the past decade, the global commercial fleet's total size has increased, resulting in increased emissions that have a negative impact on the environment. GHG emissions and CO_2 as a primary source of greenhouse gases have a detrimental influence on the world agriculture and trade [2].

Green shipping and fuel-consumption reduction are mandatory for the International Maritime Organization (IMO) in the field of shipping transportation, and these issues are dealt with in Annex VI of the MARPOL 73/78 Convention on the Prevention of Pollution from Ships, which contains provisions about harmful emissions pollution prevention. The MEPC 70 also adopted a GHG reduction plan roadmap for establishing a comprehensive IMO GHG strategy. This anticipated the April 2018 approval of a preliminary emission reductions strategy [3],[4].

IMO has completed implementing EEDI by targeting ships which use the most fuel in the marine fleet. Thus, 72% of the commercial fleet is made energy efficient with this purpose [5]. As of January 1, 2013, EEDI deployments have begun, and energy efficiency strategies have been developed every five years to account for emerging technology in this sector [6]. Figure 1 depicts the timeline for the installation of the EEDI system. In the first stage, energy efficiency is expected to be 10 percent, with the goal of increasing it to 30 percent by 2030. By 2050, it is anticipated that this ratio would have increased to 50 percent.

* Corresponding author

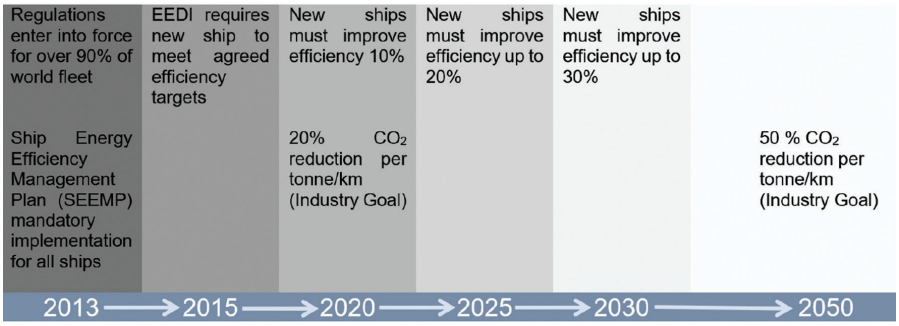

Figure 1 EEDI implementation schedule [7]
Slika 1. Raspored primjene EEDI-a [7]

Many efforts to reduce total ship resistance and hence the power in a feasible and practical manner have been conducted worldwide in the last 40 years. Lindstad et. al. [8] observes the critical nature of using suitable engine technology to achieve the greatest possible reductions in GHG emissions. Following that, Farkas et al. [9] calculated the fuel savings and CO_2 emissions reductions that could be achieved by using antifouling coatings with decreased roughness on crude oil and bulk carriers as examples. A speed reduction of 13.6% for an engine driven by low sulphur marine gas oil resulted in significant savings in fuel oil consumption and CO_2 emissions for all sea states studied. Steam turbines can save much more fuel. Using liquefied natural gas instead of low sulphur marine gas oil can save up to 49% of CO_2 emissions [10]. The use of non-carbon fuels has the greatest mitigation potential, but has seen the least implementation too far. The other two solutions with strong mitigation potential are already well adopted by the market and should not be installed anew in a meaningful proportion of the fleet [11]. Other work was summarized by Molland et al. [12] including improving the efficiency of propulsors and reducing total vessel resistance. The later can be achieved by improving ship hull design and changing monohull into multihull vessels such as in the form of catamaran and trimaran.

Over the last four decades, the usage of multihull ships for a variety of purposes has increased significantly, including ferries, fishing vessels, sports ships, and oceanographic research vessels [13]. The obvious benefits of these vessels over monohull vessels include more appealing layout accommodations, improved transverse stability, and in some cases, the possibility to reduce overall resistance and therefore the size of the main engine, thereby decreasing CO_2 pollution in the air and lowering the EEDI [14]. Numerous vessel types are further developed to meet the design parameters. Among others, the catamaran and trimaran concepts are favoured and gaining popularity. As noted before by Molland et al.[13], the catamaran concept garnered great interest since it allows for a larger deck surface while retaining transverse stability. Meanwhile, the trimaran hull shape, or ship with three hulls, has gained popularity as a result of its ability to give a larger deck area and superior seakeeping qualities in comparison to the catamaran [15].

Trimaran resistance may be complicated for ship designers, especially when the sidehull and mainhull interact. For proper calculations based on scaling from model to real ship, it is essential to grasp the breakdown and knowledge of right ship resistance components. The Resistance components of multihull ships are more complicated than those of monohull vessels, due to the complexity of the interference effect caused by the interaction between the hulls of a multihull ship. The resistance and powering characteristics of a trimaran, as well as the influence of outrigger hull shapes, were investigated using calculation and experiment approaches [16]. It has been found that the strength of cross flow is linked to the resistance to interference [17],[18]. Hu et al. [19] identified that certain hull layouts can effectively reduce wave resistance at various Froude numbers. Uithof et al. [20] conducted a thorough study that revealed a distinct separation between the sidehull and mainhull, resulting in minimal or no contact. The minor interaction occurs between S/L 0.4 and 0.5, implying that a trimaran with equivalent displacement to a monohull might have lower resistance and main engine power. The resistances and powering characteristics of a trimaran, as well as the influence of outrigger hull shapes, were investigated using numerical and experimental approaches.

The improvement of resistance through hull optimization is later carried out using Axe-Bow concept [21]. Axe-Bow uses straight vertical sides in the extended section as an empty space. It is effective to diminish waves from the bow, thus it causes a smoother pitching motion and can reduce the use of fossil fuels. The use of Axe-Bow developed by Damen Shipyard has demonstrated efficiency and better head sea performance with less slamming and higher speeds [22]. Later, Damen Shipyard [23] made a historic delivery of the first ship (i.e. a patrol boat) with Axe-Bow. The ship unveils effective movement behaviour and significant lower resistance when sailing in open sea and delivers approximately 20% reduction in fuel use and hence decreases the emission of toxic gases. Recent work carried out by Utama et al. [24] supports the advantages of using Axe-Bow. Monohull with Axe-Bow has reduced total resistance by about 11%, whereas the reduction in trimaran mode is approximately 8%. Lower reduction in the latter case is attributed to the interference effect between main-hull and side-hulls of the trimaran.

The main objective of the study is to analyse the EEDI of trimaran configuration without and with Axe-Bow and compared against monohull type with similar displacement. A monohull cargo vessel called MVSabuk Nusantara 104, operated in Maluku waters in the last 4 years, was used for comparative purposes. The calculation was made in accordance with the IMO regulations. Furthermore, the contribution of the study is to provide and strengthen the use of multihull vessels to limit EEDI of operational vessels and hence develop more environmentally friendly sea transportation. In addition, it is closely tied to ship-associated air pollution.

2. METHODS / *Metode*

2.1. Trimaran Model / *Model trimarana*

The investigation was carried out by using trimaran NPL4a model, both with and without Axe-Bow, and MVSabuk Nusantara 104, as illustrated in Figures 2 - 4, with the most important details being included in Table 1.

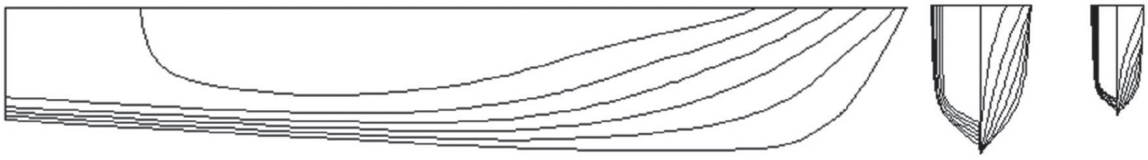

(a) Sheer plan / *Uzdužni presjek broda* (b) Body plan / *Nacrt linija broda*

Figure 2 NPL 4a without Axe-Bow
Slika 2. NPL 4a bez sjekirastog pramca

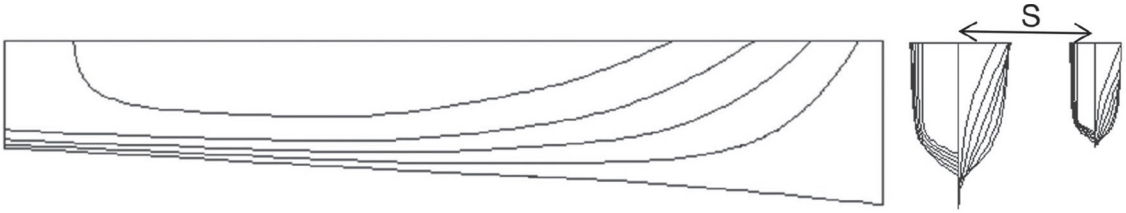

(a) Sheer plan / *Uzdužni presjek broda* (b) Body plan / *Nacrt linija broda*

Figure 3 NPL 4 with Axe-Bow
Slika 3 NPL 4 sa sjekirastim pramcem

(a) Sheer plan / *Uzdužni presjek broda* (b) Body plan / *Nacrt linija broda*

Figure 4 MV Sabuk Nusantara 104 [25]
Slika 4. MV Sabuk Nusantara 104 [25]

Table 1 Principal Particular of the models
Tablica 1. Osnovni podaci modela

Parameter	Unit	Trimaran without Axe-Bow		Trimaran with Axe-Bow		MV. Sabuk Nusantara 104
		Mainhull	Sidehull	Mainhull	Sidehull	
Length (L)	m	1.252	1.058	1.252	1.058	1.030
Breadth (B)	m	0.168	0.168	0.096	0.168	0.197
Separation between the centerlines of mainhull and sidehull (S)	m	0.376 at S/L=0.3 0.501 at S/L=0.4				-
Height at Main Deck (H)	m	0.121		0.121		0.066
Draught (T)	m	0.067		0.096		0.045
Wetted Surface Area (WSA)	m	0.398		0.418		0.402
Displacement ()	kg	6.943		6.943		6.943
Coefficient Block (Cb)		0.356		0.323		0.726

2.2. Resistance / *Otpor*

Computational Fluid Dynamics (CFD) technique was used to predict the resistance of models. Sahid and Huang [26] have carried out research on calculating the hull resistance of trimaran ships by using CFD, which showed good results. The Reynolds-averaged Navier-Stokes (RANS) method is a three-dimensional equation developed and was used in the CFD model. The flow problem in the walls of a ship is solved using unsteady incompressible flow provided by ANSYS-CFX [27].

In the modeling of wake fields, it is discovered that the selection of turbulence models is very important. This study makes use of the SST (Shear Stress Transport) turbulence model created by Menter [28]. The SST model has been utilized and verified by many researchers, all of whom have had positive findings using the model [29]. The RANS solver, which is implemented in ANSYS CFX, is used to solve the fluid flow field. Equations (1), (2), and (3) illustrate the continuity, RANS, and SST turbulence equations, respectively, as follows :

Continuity equation:

$$\frac{\partial \rho}{\partial t} + \frac{\partial}{\partial x_j}(\rho U_j) = 0 \quad (1)$$

Where: ρ is fluid density, t is time, U_j is the flow velocity vector field.
RANS equation:

$$\rho \bar{f}_i + \frac{\partial}{\partial x_j}\left[-\bar{p}\delta_{ij} + \mu\left(\frac{\partial \bar{u}_i}{\partial x_j} + \frac{\partial \bar{u}_j}{\partial x_i}\right) - \overline{\rho u_i' u_j'}\right] - \rho \bar{u}_j \frac{\partial \bar{u}_i}{\partial x_j} = 0 \quad (2)$$

The left side of RANS equation represents the change in mean momentum of fluid element to the unsteadiness in the mean flow. This change is balanced by the mean body force ($\bar{f}_i$), the mean pressure field ($\bar{p}$), the viscous stress, $\mu\left(\frac{\partial \bar{u}_i}{\partial x_j} + \frac{\partial \bar{u}_j}{\partial x_i}\right)$, and apparent stress ($\rho u_i' u_j'$) to the fluctuating velocity field.
Menter's SST equation

$$\frac{\gamma}{\nu_t} P - \beta \rho \omega^2 + \frac{\partial}{\partial x_j}\left[(\mu + \sigma_\omega \mu_t)\frac{\partial \omega}{\partial x_j}\right] + \\ + 2(1 - F_1)2\rho_{\omega 2}\frac{1}{\omega}\frac{\partial k}{\partial x_j}\frac{\partial \omega}{\partial x_j} - \left(\frac{\partial(\rho\omega)}{\partial t} + \frac{\partial(\rho u_j \omega)}{\partial x_j}\right) = 0 \quad (3)$$

The Menter's SST model combines the advantages of the *k-ω* model to achieve an optimal model formulation for a wide range of applications. For this, a blending function *F1* is introduced which is equal to one near the solid surface and equal to zero for the flow domain away from the wall. It activates the *k-ω* wall region and the *k-ε* model for residual flow. By this approach, the attractive near-wall performance of the *k-ω* model can be used for the free stream sensitivity.

2.3. Numerical Domain and Boundary Setting / *Numerička domena i zadavanje rubnih uvjeta*

The most recommended computational domain at velocity inlet was set 2L forward perpendicular to the front and at the outlet pressure it was 5L towards the back which was measured perpendicularly. To eliminate the effect of backward flow on side boundaries, the transverse and vertical directions were set at 2L-3L [30].

Figure 5 depicts the domain dimensions as well as the boundary conditions, as follows: the hull body is defined as a fixed boundary, and a no-slip condition is imposed on the model; a free-slip condition is applied to the bottom; an opening condition was applied to the top wall, and a symmetry condition was used for the side walls; the flow velocity at the inlet is defined as Fr = 0.15 to 0.5; the hydrostatic pressure at the outlet is defined as a function of water level; the flow velocity at the inlet is defined as Fr. The starting position of the free surface is also defined by specifying the volume fraction function of water and air at the input and exit of the system.

2.4. Grid Generation / *Generiranje mreže*

The mesh creation was done with ANSYS DesignModeler. The computation domain is unstructured with inflation mesh (Figure 6). Due to the model's complicated geometry, a triangular mesh is produced on the model's surface, and the boundary layer is refined with prism components. Inflation fills the area around the model with tetrahedral components.

Grid independence analysis was carried out to determine the most appropriate element size for the numerical analysis. A higher resolution mesh can always produce realistic results in CFD, but the enormous element number increases the computational cost and time consumption. Mesh convergence investigations were carried out for the trimaran and MV Sabuk Nusantara 104 models hull at Froude number of 0.2. In order to evaluate the resistance of ship models, several grid sizes ranging from 160 thousand to 3.5 million elements were used to evaluate them. Grid independence study was shown in Figure 7. It was discovered that there was no substantial variation (less than 2 percent) [31] in resistance beyond the grid size of 1.2 million for trimaran without Axe-Bow, 1.3 million for trimaran with Axe-Bow, and 1.9 million for MV Sabuk Nusantara 104 when the grid size was increased. As a result, for the numerical simulation, the grid size that has been previously determined

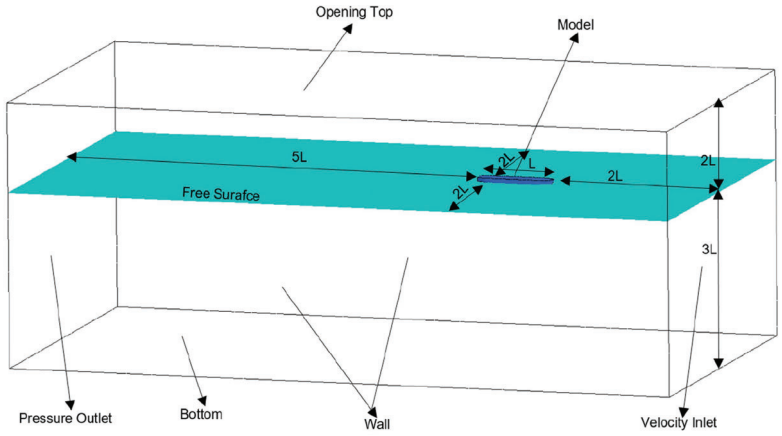

Figure 5 Boundary Conditions
Slika 5. Rubni uvjeti

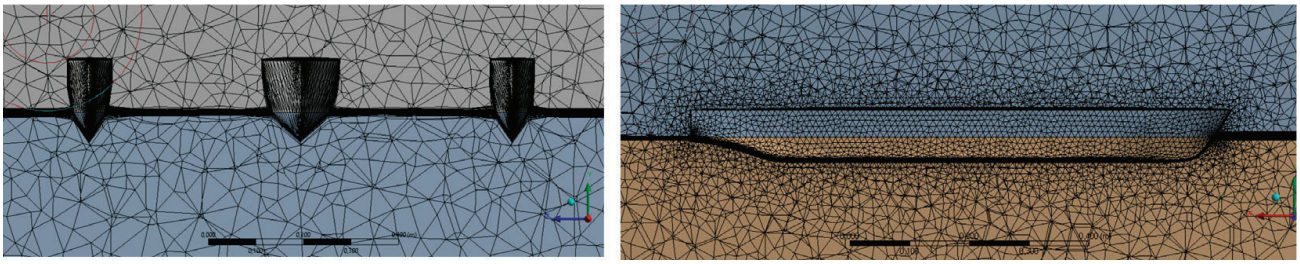

(a) Trimaran Hull / Trup trimarana (b) MV. Sabuk Nusantara 104 / MV Sabuk Nusantara

Figure 6 Unstructured mesh with inflation
Slika 6. Nestrukturirana mreža s diskretiziranim graničnim slojem

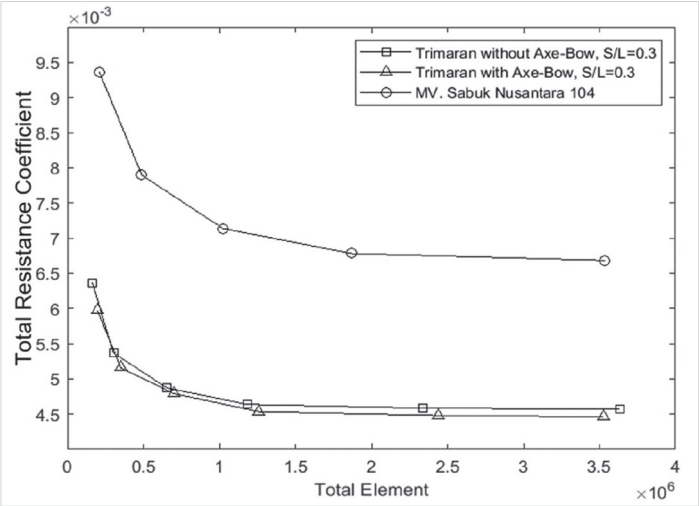

Figure 7 Grid Independence Study
Slika 7. Analiza utjecaja gustoće mreže

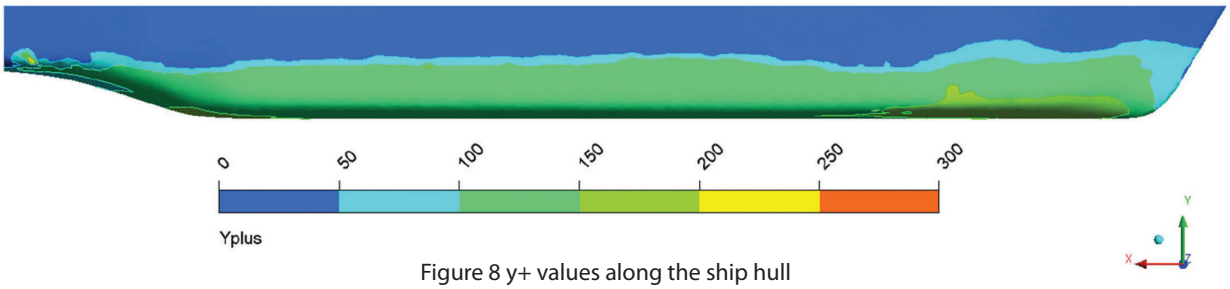

Figure 8 y+ values along the ship hull
Slika 8. y+ vrijednosti na trupu broda

has been utilized to run the entire simulations at varying speeds, as previously stated.

A high aspect ratio layer is applied into an isotropic cell subdivision to provide sufficient resolution for the flow. For cells located near the wall, it is required to account for fluctuations in the wall y+, as shown in equation (4)

$$y^+ = \frac{\rho u_\tau y_{wall}}{\mu} \quad (4)$$

The accuracy of the computations in the region near the wall is critical for the simulation's effectiveness. Wall functions use the predictable dimensionless boundary layer profile described on the previous slide to determine the wall conditions (e.g. shear stress) based on where the centroid of the wall adjacent mesh cell is in the log-layer. CFD simulation on ships under draft that has been carried out obtains a value of y+ <300 (Figure 8). This is in accordance with the normally the first cell in the log-layer that should have 30 <y+<300. This is a fairly broad guideline; y+ can be larger if still in the log layer and for very low values (but still turbulent) In addition, the log-layer may not extend far enough away from the wall for the use of wall functions to be valid [27].

2.5. EEDI (Energy Efficiency Design Index) / *Projektni indeks energetske učinkovitosti*

EEDI (Energy Efficiency Design Index) is a proposed piece of legislation by the International Maritime Organization (IMO) that would allow ships to be measured for their energy efficiency. In the ship design process, the EEDI index is used to determine the amount of CO_2 emissions created per unit of ship travel. The lower the ship's EEDI index, the lower the amount of CO_2 emissions. EEDI is calculated using a complicated algorithm that takes into consideration the ship's emissions, capacity, and speed. In accordance with the definition of EEDI provided by the ICCT (International Council on Clean Transportation) [32], it may be estimated using the following equation (5):

$$EEDI = \frac{P*SFC*CF}{C*v} \text{ gm } CO_2/\text{tonne.mile} \quad (5)$$

In Equation (4), P is the independent engine power at 75% of MCR (kW), C is the CO_2 emission determined the association on the fuel type that was used by provided engine, (t-CO_2/t-Fuel), SFC is the specific fuel consumed per unit of engine power, as certified by the manufacturer, (g/kWh), f is the non-dimensional factors which were added to the EEDI approximation to profile for several specific present system, and v_{ref} is the service speed at maximum load (knot), c is the capacity in deadweight tonnage (DWT) or Gross Tonnage (GT).

Deadweight was used as a capacity for calculations of EEDI for general cargo vessels & oil tankers. On the other hand, for passenger vessels GT was considered for capacity, as suggested by IMO. It is important to underline that the calculation of EEDI within this analysis wase performed with 75% of MCR, which was recommended by the IMO, and with the corresponding evaluated maximum ship speed. Furthermore, the value of SFC for main engines of seagoing vessels is 220 g/kWh, which is the

estimated average value of ship engines powered by diesel fuel [33]. The adopted value of carbon emissions factor (CF) for diesel fuel was 3.2 t CO_2/t fuel, as recommended in IMO 2010 [6], and can be seen in Table 2.

The measured EEDI of a ship is referred to as the achieved EEDI. The achieved EEDI must be smaller than the reference EEDI line. The values of the reference lines were computed as follows (equation 6):

$$\text{Reference line value} = ab^{-c} \quad (6)$$

Where a, b and c are the parameters given in Table 3.

In this paper, a study was conducted on MV Sabuk Nusantara 104, as shown in Figure 9, which operated in the waters of Kupang (NTT) – Saumlaki (Maluku) with IMO number: 9813785 and registered with Indonesian Classification Bureau (BKI) [34]. The ship was built in 2017, it belongs to the Ministry of Sea Transportation of the Republic of Indonesia and its particulars are presented in Table 4.

Table 2 Carbon content and CF values of different types of fuel (IMO, 2016)
Tablica 2. Sadržaj ugljika i CF vrijednosti različitih vrsta goriva (IMO, 2016.)

Type of fuel	Reference	Carbon Content	CF (t-CO2/t-Fuel)
Diesel / Gas Oil	ISO 8217 Grades DMX through DMB	0.874	3.206
Light Fuel Oil (LFO)	ISO 8217 Grades RMA through RMD	0.859	3.151
Heavy Fuel Oil (HFO)	ISO 8217 Grades RME through RMK	0.849	3.114
Liquefied Natural Gas ((LNG)		0.750	2.750
Methanol		0.375	1.375
Ethanol		0.522	1.913

Table 3 Reference line value (a, b, and c) parameters (the reference EEDI) (IMO, 2016)
Tablica 3. Parametri vrijednosti referentne linije (a, b i c) (referentni EEDI) (IMO, 2016.)

Ship type defined in regulation	a	b	c
Bulk carrier	961.79	DWT	0.477
Tanker	1218.8	DWT	0.488
General cargo ship	107.48	DWT	0.216
Combination carrier	1219	DWT	0.488
Roro cargo ship	1405.15	GT	0.5
Roro passenger ship	752.16	GT	0.38

Figure 9 MV. Sabuk Nusantara 104
Slika 9. MV Sabuk Nusantara 104

Table 4 Particular Data of MV Sabuk Nusantara 104
Tablica 4. Podaci MV Sabuk Nusantara 104

Parameter	Value
Flag	Indonesia
IMO No	9813785
Length	57.36 m
Breadth	12.00 m
Draught	2.70 m
Gross Tonnage	1259 GT
Main Engine Type	Yanmar
Main Engine Power	1673 kW
Service Speed	10 knots
Passenger Capacity	476 persons
Cargo Capacity	150 Ton

3. RESULTS AND DISCUSSION / *Rezultati i rasprava*

3.1. Resistance of Ship Models / *Otpor modela brodova*

The results of ship model calculation by using CFD approach are shown in Figure 10. All trimaran models have a lower drag coefficient than the MV Sabuk Nusantara 104 model with an average difference of 50.24%. This decrease in ship resistance was significant, which was due to the slimmer hull shape of the trimaran compared to the MV Sabuk Nusantara 104, as shown in Figures 11 to 15.

Furthermore, the trimaran vessel with Axe-Bow shows a smaller value than the trimaran without Axe-Bow hull. This is due to the introduction of the Axe-Bow which can reduce wave generation around the ship, as shown Figures 11 to 14. The use of Axe-Bow can reduce the resistance by about 3.80% compared with trimaran without Axe-Bow.

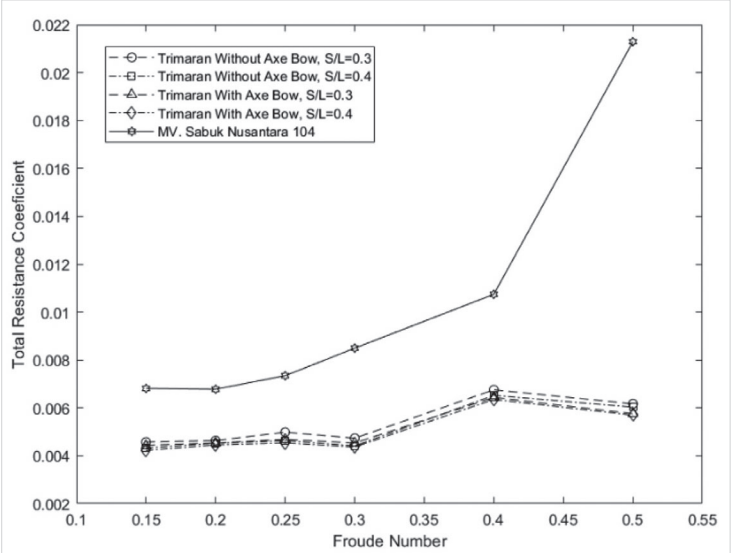

Figure 10 Total Resistance Coefficient of Ship Models
Slika 10. Koeficijent ukupnog otpora modela brodova

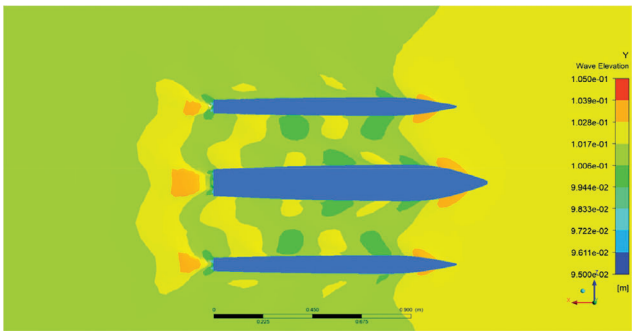

Figure 11 Wave Elevation around Trimaran without Axe-Bow, S/L=0.3 at Fr= 0.2
Slika 11. Elevacija valova oko trimarana bez sjekirastog pramca, S/L=0,3 pri Fr= 0,2

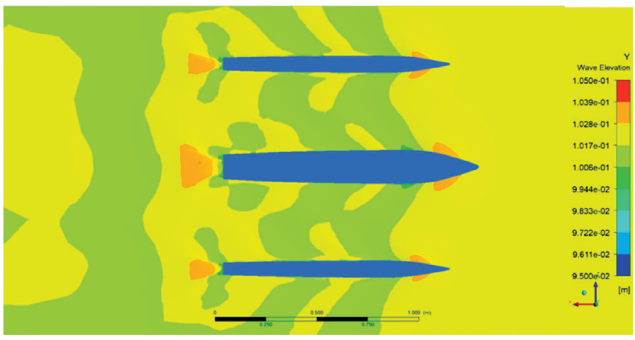

Figure 12 Wave Elevation around Trimaran without Axe-Bow, S/L=0.4 at Fr= 0.2
Slika 12. Elevacija valova oko trimarana bez sjekirastog pramca, S/L=0,4 pri Fr= 0,2

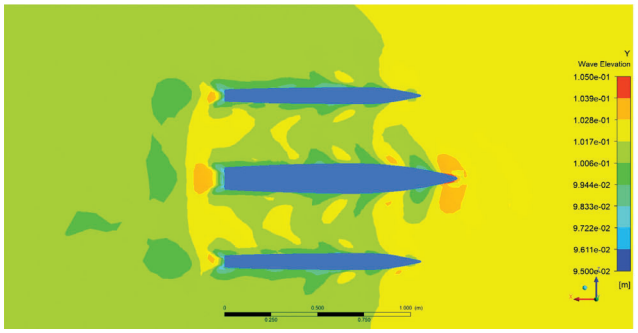

Figure 13 Wave Elevation around Trimaran with Axe-Bow, S/L=0.3 at Fr= 0.2 /
Slika 13. Elevacija valova oko trimarana sa sjekirastim pramcem, S/L=0,3 pri Fr= 0,2

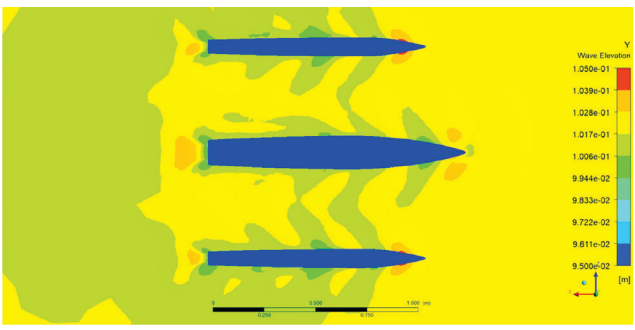

Figure 14 Wave Elevation around Trimaran with Axe-Bow, S/L=0.4 at Fr= 0.2 /
Slika 14. Elevacija valova oko trimarana sa sjekirastim pramcem, S/L=0.4 at Fr= 0.2

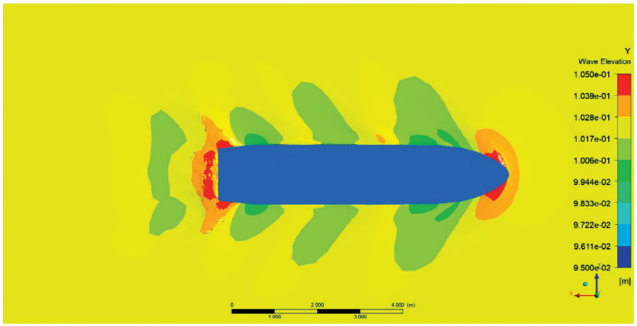

Figure 15 Wave Elevation around MV Sabuk Nusantara at Fr= 0.2
Slika 15. Elevacija valova oko MV Sabuk Nusantara pri Fr= 0,2

The flow of water on a trimaran without Axe-Bow shows a significant interaction between the hulls at the variation of S/L=0.3 in Figure 11, then the interaction decreases in the variation of the trimaran with S/L=0.4, as shown in Figure 12, which indicates an increase in resistance. Meanwhile, the interaction of water flow in the trimaran hull with Axe-Bow hull was not significant as shown in Figures 13 and 14.

Furthermore, MV Sabuk Nusantara 104 shows a fairly high water flow at fore and along the hull ship region, as shown in Figure 15. The interaction of water and ship hull causes an increase of resistance. The visualization of flow velocity around hull shows the cause of ship resistance increase. This phenomenon explains that the trimaran ship with axe- bow has less resistance than other ship models that have been analyzed by CFD.

3.2. Full-Scale Ship Resistance Estimation / *Procjena otpora broda u naravi*

The ship's full-scale calculation is based on the same displacement data, which is obtained through the calculation of MV Sabuk Nusantara 104 particular dimension [25] with a scale of 1:61, by using the equation (6) below:

$$\frac{1}{\lambda} = \frac{\rho_{Model}}{\rho_{Ship}} \left(\frac{\nabla_{Model}}{\nabla_{Ship}} \right)^{\frac{1}{3}} \quad (7)$$

Where, ∇ is displacement (kg) and λ is scale factor.

All ship models are assumed to have Gross Tonnage (GT) which is proportional to the displacement of a ship, thus a full-scale ship will be obtained as shown in Table 5.

Furthermore, the calculation of the full-scale ship resistance used the Froude extrapolation method. This method uses the help of the coefficient of total resistance (C_T) [13], which is shown in equation; the full-scale resistance of the ship is obtained by the formula as written in equation (7) below:

$$C_T^M = \frac{R_T^M}{0.5\rho v_m^2 WSA_M} \quad (8)$$

$$C_T^S = \frac{R_T^S}{0.5\rho v_s^2 WSA_S} \quad (9)$$

then,

$$C_T^M = C_T^S \quad (10)$$

Where:
C_T^M is total resistance coefficient of model
C_T^S is total resistance coefficient of ship
R_T^M is total resistance of model (N)
R_T^S is total resistance of ship (kN)
v_M is velocity of model (m/s)
v_S is velocity of ship (m/s)
WSA_M is wetted surface area of model (m^2)
WSA_S is wetted surface area of ship (m^2)

In practice, a correction factor (Correlation Allowance) is required to account for effects not considered by Froude's assumptions. However, it is ignored in this research because the total efficiency () is calculated during the power calculation. Figure 16 illustrates the calculation of full-scale resistance using Froude extrapolation.

Table 5 Dimension Full-Scale of Ships
Tablica 5. Dimenzije broda u naravi

Parameter	Unit	Trimaran without Axe-Bow	Trimaran with Axe-Bow	MV. Sabuk Nusantara 104
Length Over All (LOA)	m	76.372	76.372	62.830
Length Water Line (LWL)	m	74.298	76.372	57.340
Breadth (B)	m	0.848 at S/L=0.3		0.197
		1.098 at S/L=0.4		
Height (H)	m	7.381	7.381	4.026
Draft (T)	m	4.087	5.856	2.745
Wetted Surface Area (WSA)	m^2	1,480.958	1,555.378	1,495.842
Displacement ()	Ton	1,575.929	1,575.929	1,575.929
Gross Tonnage (GT)		1,259	1,259	1,259
Cb		0.356	0.323	0.726

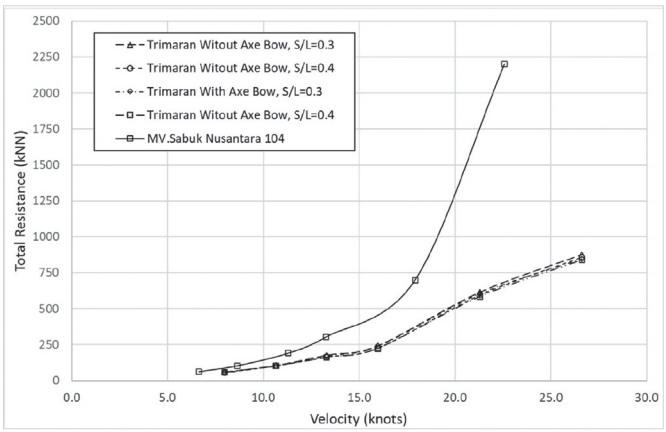

Figure 16 Total Ship Resistance
Slika 16. Ukupni otpor broda

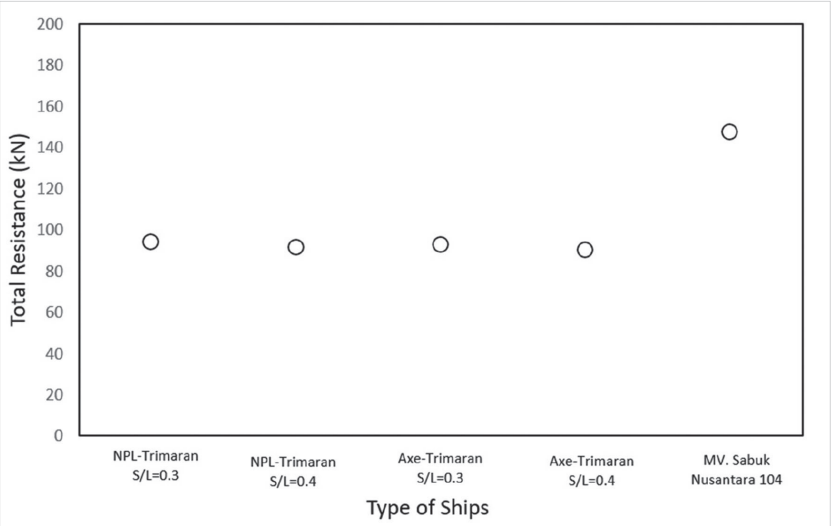

Figure 17 Total Resistance of Ship at 10 knots
Slika 17. Ukupni otpor broda pri brzini od 10 čvorova

The calculation of the resistance of the ships at 10 knots is carried out by linear interpolation with the equation (11). The results of total resistance of the full-scale ship show that all ship models have almost the same resistance up to a speed of 10 knots, where the trimaran vessel has a smaller resistance than the MV Sabuk Nusantara with an average difference of about 37.51%. Furthermore, MV Sabuk Nusantara 104 has a very high resistance increase compared to the other ships at speeds more than 10 knots and it is very ineffective to operate at these speeds, as shown in Figure 17.

$$\frac{v_s - v_1}{v_2 - v_1} = \frac{R_{T_s} - R_{T_1}}{R_{T_2} - R_{T_1}} \tag{11}$$

3.3. Power Calculation of Ship / *Izračun snage broda*

The power value of the ship has a significant impact on the EEDI measurement. Calculation of the power of the ship using equations 11 and 12 [13]. Both equations are intended to obtain the total efficiency of power. As a basis for calculating efficiency, resistance data and machines installed with MV Sabuk Nusantara 104 were used so that the engine efficiency is obtained by 43.96%. Furthermore, the calculation of the power of each ship is carried out using the efficiency value, as shown at Figure 18.

$$\begin{aligned} P_E &= R_T * v_s \\ &= 143.08 * 5.14 \\ &= 735.42 \end{aligned} \tag{12}$$

where:
P_E is Effective Power (kW)
R_T is Total Resistance (kN)
v_s is Service Speed (m/s)

Then,

$$\begin{aligned} \eta_T &= \frac{P_E}{P_B} \\ &= \frac{735.42}{1673} \\ &= 43{,}96\% \end{aligned} \tag{13}$$

where:
P_B is Brake Power (kW)
η_T is Total Power Efficiency

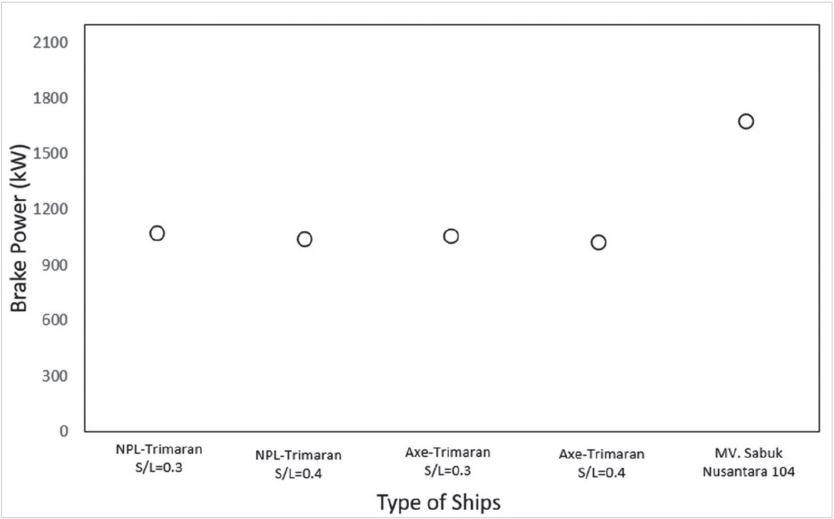

Figure 18 Brake Power of ships at 10 knots
Slika 18. Kočena snaga brodova pri brzini od 10 čvorova

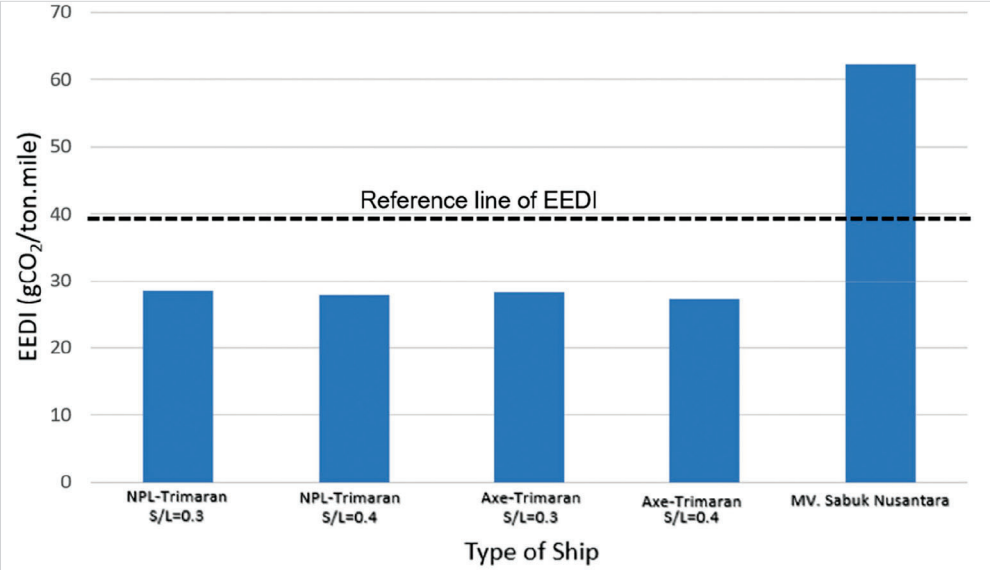

Figure 19 EEDI of Ships
Slika 19. EEDI brodova

3.4. EEDI Calculation of Ship / *EEDI izračun broda*

The reference EEDI and the achieved EEDI of the ship were determined using equations 4 and 5 based on the collected data. Table 3 shows the value of the ship's reference line where the value of "a" is 1405 GT, "c" is 0.5 while the value of "b" refers to Table 4 which is 1259 GT. The ship under investigation is a passenger/ro-ro cargo ship, and its specifications are as follows:

Reference line of EEDI $= 1405*1259^{-0.5}$
$= 39.6\ gCO_2/ton\text{-}mile$

The MV Sabuk Nusantara 104 operates at service speed of 10 knots and has Yanmar engine with 1673 kW. The comparison between ships at the same speed is obtained. The EEDI formula for each ship is shown in Figure 19.

The trimaran model has a better estimate of EEDI calculation than the MV Sabuk Nusantara 104 with an average difference of 55.1%, as shown in Figure 18. This shows that the trimaran hull mode has better performance than the MV Sabuk Nusantara 104 vessel. The Analysis and Calculation demonstrate that the MV Sabuk Nusantara 104 exceeds the Reference line of EEDI, while the trimaran ship model has an EEDI that is below the Reference line of EEDI. This indicates that the trimaran vessel has a more environmentally friendly performance than the MV Sabuk Nusantara 104 Vessel.

4. CONCLUSIONS / *Zaključci*

A study into the effect of using axe-bow on trimaran hull has been carried out numerically using the CFD approach and has shown the effectiveness of introducing axe-bow on the main hull of trimaran to further reduce the total drag of the trimaran. Furthermore, the use of axe-bow has demonstrated very well on the reduction of CO_2 emission which is termed as EEDI.

A comparative study using a monohull cargo/passenger ship with similar displacement showed that trimaran with axe-bow can decrease significantly the total resistance and EEDI. The conclusions are as follows:

- The trimaran total resistance without and with axe-bow showed the reduction of 22.6% and 25.0%, respectively, compared to the total resistance of MV Sabuk Nusantara 104, a monohull with similar displacement. This further indicated that the introduction of axe-bow can decrease the total resistance by about 2.4%.
- The use of trimaran without and with axe-bow can reduce EEDI by about 54.8% and 55.4%, respectively, compared to the EEDI of monohull with comparable displacement. It can be said that the use of axe-bow can lower EEDI by more than 0.6%.

Acknowledgment / *Zahvala*

The authors thank the University of Pattimura for funding the research project under contract number 1999/UN13/SK/2020. The third author acknowledges the support from the Institute Technology of Sepuluh Nopember under postgraduate research funding with contract number: 920/PKS/ITS/2020.

REFERENCE / *Literatura*

[1] UNCTAD. (2018). Reveiw of Maritime Transport. In United Nations Conference on Trade and Development. https://unctad.org/en/PublicationsLibrary/rmt2018_en.pdf

[2] Nunex, C. (2019). Carbon dioxide levels are at a record high. Here's what you need to know. National Geographic, 1-15. https://www.nationalgeographic.com/environment/global-warming/greenhouse-gases

[3] IMO. (2013). Greenhouse Gas Emissions. January 2013. https://www.imo.org/en/OurWork/Environment/Pages/GHG-Emissions.aspx

[4] IMO. (2021). Roadmap For Developing A Comprehensive IMO Strategy On Reduction Of GHG Emissions From Ships-MEPC 70/18/Add.1-Annex 22. January 2019, 6.

[5] Singhal, C., & Dev, A. (2013). SEEMP: Energy Management and the Shipping Industry. 69-75. https://doi.org/10.3850/978-981-07-7338-0_OSV2013-06

[6] IMO. (2016). IMO Train the Trainer (TTT) Course on Energy Efficient Ship Operation. International Maritime Organization, January, 1-59.

[7] Tokuslu, A. (2020). Energy Efficiency of a Passenger Ship in Turkey. Scientific Bulletin of Naval Academy, 23(1), 1-8. https://doi.org/10.21279/1454-864X-20-I1-002

[8] Lindstad, E., Eskeland, G. S., Rialland, A., & Valland, A. (n.d.). Decarbonizing Maritime Transport: The Importance of Engine Technology and Regulations for LNG to Serve as a Transition Fuel. https://doi.org/10.3390/su12218793

[9] Farkas, A., Degiuli, N., Martić, I., & Vujanović, M. (2021). Greenhouse gas emissions reduction potential by using antifouling coatings in a maritime transport industry. Journal of Cleaner Production, 295, 126428. https://doi.org/10.1016/j.jclepro.2021.126428

[10] Degiuli, N., Martić, I., Farkas, A., & Gospić, I. (2021). The impact of slow steaming on reducing CO_2 emissions in the Mediterranean Sea. Energy Reports, 7, 8131-8141. https://doi.org/10.1016/j.egyr.2021.02.046

[11] Nepomuceno de Oliveira, M. A., Szklo, A., & Castelo Branco, D. A. (2022). Implementation of Maritime Transport Mitigation Measures according to their marginal abatement costs and their mitigation potentials. Energy Policy, 160, 112699. https://doi.org/10.1016/j.enpol.2021.112699

[12] Molland, A.F., Turnock, S. R., Hudson, D. A., & Utama, I. K. A. P. (2014). Reducing Ship Emissions: A Review of Potential Practical Improvements in The Propulsive Efficiency of Future. Transaction RINA: IJME 156, A2, 175.https://doi.org/10.5750/ijme.v156iA2.925

[13] Molland, Anthony F., Turnock, S. R., & Hudson, D. A. (2017). hip Resistance and Propulsion: Practical Estimation of Ship Propulsive Power 2nd Edition (2nd ed.). Cambridge University Press. https://doi.org/10.1017/9781316494196

[14] Luhulima, R. B., Sutiyo, & Utama, I. K. A. P. (2017). An Investigation into The Correlation Between Resistance and Seakeeping Characteristics of Trimaran at Various Configuration and with Particular Case in Connection with Energy Efficiency. Proceedings of the International Symposium on Marine Engineering (ISME) October 15-19, 2017, Tokyo, Japan.

[15] Luhulima, R. B., Setyawan, D., & Utama, I. K. A. P. (2014). Selecting Monohull, Catamaran and Trimaran as Suitable Passenger Vessels Based on Stability and Seakeeping Criteria. The 14th International Ship Stability Workshop (ISSW), 29 September-01 October 2014, Malaysia.

[16] Degiuli, N., Werner, A., & Zotti, I. (2005). An Experimental Investigation into The Resistance Components of Trimaran Configurations. International Conference on Fast Sea Transportation, Russia.

[17] Farkas, A., Degiuli, N., & Martić, I. (2017). Numerical investigation into the interaction of resistance components for a series 60 catamaran. Ocean Engineering, 146, 151-169. https://doi.org/10.1016/j.oceaneng.2017.09.043

[18] Utama, I. K. A. P., Aryawan, W. D., Nasirudin, A., Sutiyo, & Yanuar. (2021). Numerical Investigation into the Pressure and Flow Velocity Distributions of a Slender-Body Catamaran Due to Viscous Interference Effects. International Journal of Technology, 12(1), 149. https://doi.org/10.14716/ijtech.v12i1.4269

[19] Hu, J., Zhang, Y., Wang, P., & Qin, F. (2020). Numerical And Experimental Study On Resistance Of Asymmetric Catamaran With Different Layouts. 71, 2020. https://doi.org/10.21278/brod71206

[20] Uithof, K., Oossanen, P. G. van, & Bergsma, F. (2015). The Feasibility And Performance Of A Trimaran Yacht Concept Equipped With A Hull Vane. Acta Universitatis Agriculturae et Silviculturae Mendelianae Brunensis. https://doi.org/10.1377/hlthaff.2013.0625

[21] Gelling, J. L. (2006). the Axe Bow: the shape of Ships to Come. International HISWA Symposium on Yacht Design and Yacht Construction, 19th. Amsterdam, NL, 13-14 November 2006.

[22] Buckley, T. (2010). The Axe Factor : Damen dan Amels Take a Bow. The Yatch Report, 111.

[23] Damen Shipyard. (2012). P511-Guardião: Damen Shipyard's first full axe-bow patrol vessel delivered to Cape Uerdean coast guard. Maritime by Holland.

[24] Utama, I. K. A. P., Sutiyo, & Suastika, I. K. (2021). Experimental and Numerical Investigation into the Effect of the Axe-Bow on the Drag Reduction of a Trimaran Configuration. International Journal of Technology, 12(3), 527-538. https://doi.org/10.14716/ijtech.v12i3.4659

[25] Ministry of Sea Transportation of the Republic of Indonesia. (2019). Ship Specifications: MV. Sabuk Nusantara 104.

[26] Shahid, M., & Huang, D. (2011). Resistance calculations of trimaran hull form using computational fluid dynamics. Proceedings - 4th International Joint Conference on Computational Sciences and Optimization, CSO 2011. https://doi.org/10.1109/CSO.2011.225

[27] ANSYS. (2020). ANSYS CFX-Solver Theory Guide. Ansys Inc.

[28] Menter, F. R. (1993). Zonal two equation κ-ω turbulence models for aerodynamic flows. AIAA 23rd Fluid Dynamics, Plasmadynamics, and Lasers Conference, 1993. https://doi.org/10.2514/6.1993-2906

[29] Menter, F. R., Kuntz, M., & Langtry, R. (2003). Ten Years of Industrial Experience with the SST Turbulence Model. 4th Internal Symposium, Turbulence, Heat and Mass Transfer, 625-632.

[30] Elkafas, A. G., Elgohary, M. M., & Zeid, A. E. (2019). Numerical study on the hydrodynamic drag force of a container ship model. Alexandria Engineering Journal, 58(3), 849-859. https://doi.org/10.1016/j.aej.2019.07.004

[31] Das, P., Khan, M. M. K., Saha, S. C., & Rasul, M. G. (2016). Chapter 6 - Numerical Study of Flow Through a Reducer for Scale Growth Suppression (M. M. K. Khan & N. M. S. B. T.-T. M. for E. E. A. Hassan (eds.); pp. 119-148). Academic Press. https://doi.org/10.1016/B978-0-12-802397-6.00006-3

[32] IMO. (2014). Mepc.245(66) - 2014 Guidelines on the Method of Calculation of the Attained Energy Efficiency Design Index (Eedi) for New Ships. International Maritime Organization. http://www.imo.org/en/OurWork/Environment/PollutionPrevention/AirPollution/Documents/Air pollution/M2 EE regulations and guidelines final.pdf

[33] Endresen, Ø., Sørgård, E., Behrens, H. L., Brett, P. O., & Isaksen, I. S. A. (2007). A historical reconstruction of ships' fuel consumption and emissions. Journal of Geophysical Research Atmospheres, 112(12). https://doi.org/10.1029/2006JD007630

[34] BKI. (2018). MV. Sabuk Nusantara 104. BKI Ship Register. https://www.bki.co.id/shipregister-23255.html